MOL #99663

Title: A molecular pharmacologist's guide to GPCR crystallography.

Authors: Chayne L. Piscitelli, James Kean, Chris de Graaf, Xavier Deupi

Journal: Molecular Pharmacology

Supplemental Data

Supplementary Table 1. List of all crystallized GPCRs including the main modifications in the constructs.

Class A								
Family	Receptor	Truncation	Stabilizing Mutations	Other Mutations	Chimera	Crystallization		PDB IDs
						Tool	Method	
Amine	**β1 adrenergic** *turkey*	ΔN 3-32, ΔC 368-483, ΔICL3 244-271, 277-278	R068S, M090V, Y227A, A282L, F327A, F338M	C116L (exp.), C358A (palm.)			VD	2VT4, 2YCW, 2YCX, 2YCY, 2YCZ
		ΔN 3-32, ΔC 368-483, ΔICL3 244-271	R068S, M090V, Y227A, A282L, F327A, F338M	C116L (exp.), C358A (palm.)			VD	2Y00, 2Y01, 2Y02, 2Y03, 2Y04, 4AMI, 4AMJ, 4GPO, 3ZPR, 3ZPQ
		ΔN 3-32, ΔC 368-483, ΔICL3 244-271	R068S, M090V, Y227A, A282L, F327A, F338M, I129V, D322K, Y343L	C116L (exp.), C358A (palm.)			LCP	4BVN
	β2 adrenergic *human*	ΔC 366-413		N187E (N-gly)		Fab5	VD	2R4R
		ΔN 1-24, ΔC 366-413		N187E (N-gly)		Fab5	VD	2R4S
		ΔC 366-413, ΔICL3 234-259		N187E (N-glyc.)	T4L ICL3		LCP	2RH1
		ΔC 349-413, ΔICL3 234-259	E122W	N187E (N-glyc.)	T4L ICL3		LCP	3D4S, 3NY8, 3NY9, 3NYA
		ΔC 366-413, ΔICL3 234-259		N187E (N-glyc.)	T4L ICL3	Nb80	LCP	3P0G
		ΔN 1-23, ΔC 349-413, ΔICL3 234-259		N187E (N-glyc.), H93C (cov. lig.)	T4L ICL3		LCP	3PDS
		ΔN 1-28, ΔC 366-413, ΔICL3 235-263		N187E (N-glyc.), H93C (cov. lig.), M96T (exp), M98T (exp)	T4L N-term	Nb6B9	LCP	4QKX
		ΔN 1-28, ΔC 366-413		N187E (N-glyc.), M96T (exp.), M98T (exp.)	T4L N-term	Nb35	LCP	3SN6
		ΔN 1-28, ΔC 366-413, ΔICL3 235-263		N187E (N-glyc.), M96T (exp.), M98T (exp.)	T4L N-term		LCP	4GBR
		ΔN 1-28, ΔC 366-413, ΔICL3 235-263		N187E (N-glyc.), M96T (exp.), M98T (exp.)	T4L N-term	Nb6B9	LCP	4LDE, 4LDL, 4LDO

Class A								
Family	Receptor	Truncation	Stabilizing Mutations	Other Mutations	Chimera	Crystallization Tool	Crystallization Method	PDB IDs
Amine	**dopamine D3** *human*	ΔICL3 222-318	L119W		T4L ICL3		LCP	3PBL
	histamine 1 *human*	ΔN 1-19, ΔICL3 222-404			T4L ICL3		LCP	3RZE
	serotonin 1B *human*	ΔN 1-32, ΔICL3 240-305	L138W		bRIL ICL3		LCP	4IAR
		ΔN 1-32, ΔICL3 240-303	L138W		bRIL ICL3		LCP	4IAQ
	serotonin 2B *human*	ΔN 1-35, ΔC 406-481, ΔICL3 249-313	M144W		bRIL ICL3		LCP	4IB4, 4NC3
	M2 muscarinic acetylcholine *human*	ΔICL3 218-376		N2D (N-glyc.), N3D (N-glyc.), N6D (N-glyc.), N9D (N-glyc.)	T4L ICL3		LCP	3UON
		ΔICL3 233-374		N2D (N-glyc.), N3D (N-glyc.), N6D (N-glyc.), N9D (N-glyc.)		Nb9-8	LCP	4MQS, 4MQT
	M3 muscarinic acetylcholine *rat*	ΔN 1-56, ΔICL3 260-481			T4L ICL3		LCP	4DAJ, 4U14, 4U15, 4U16

Class A							
Family	Receptor	Truncation	Stabilizing Mutations	Other Mutations	Chimera	Crystallization Tool	Crystallization Method	PDB IDs
Peptide	**neurotensin 1** *rat*	ΔN 1-42, ΔC 397-424, ΔICL3 269-299	A86L, E166A, G215A, L310A, F358A, V360A		T4L ICL3		LCP	4GRV
		ΔN 1-49, ΔC 389-424, ΔICL3 280-295	A86L, H103D, H105Y, A161V, R167L, R213L, V234L, I253A, H305R, F358V, S362A				VD	3ZEV
		ΔN 1-49, ΔC 389-424, ΔICL3 273-290	A86L, H103D, H105Y, A161V, R167L, R213L, V234L, I253A, H305R, F358V, S362A				VD	4BUO
		ΔN 1-49, ΔC 389-424, ΔICL3 280-295	S83G, A86L, T101R, H103D, H105Y, L119F, M121L, E124D, L125V, R143K, D150E, A161V, R167L, C172R, A177H, M208V, R213L, V234L, V240L, I253A, N262R, K263R, H305R, V313M, C332V, F342A, T354S, F358V, S362A				VD	4BV0
		ΔN 1-49, ΔC 389-424, ΔICL3 280-295	S83G, A86L, T101R, H103D, H105Y, L119F, M121L, E124D, R143K, D150E, A161V, R167L, R213L, V234L, K235R, V240L, I253A, I260A, N262R, K263R, H305R, C332V, F342A, T354S, F358V, S362A				VD	4BWB
	angiotensin II type 1 *human*	ΔN 1, 7-16 ΔC 320-359			bRIL N-term		LCP	4YAY
	chemokine CCR5 *human*	ΔC 320-352, ΔICL3 224-226	C58Y, G163N, A233D, K303E		Rubredoxin ICL3		LCP	4MBS
	chemokine CXCR4 *human*	ΔC 326-352	L125W		T4L ICL3		LCP	3OE6
		ΔC 320-352	L125W		T4L ICL3		LCP	3ODU, 3OE8
		ΔC 320-352, ΔICL3 229-230	L125W	T240P (uncoup.)	T4L ICL3		LCP	3OE9, 3OE0
		ΔC 320-352, ΔICL3 229-230	L125W	T240P (uncoup.), D187C (cov. lig.)	T4L ICL3		LCP	4RWS

Class A							
Family	Receptor	Truncation	Stabilizing Mutations	Other Mutations	Chimera	Crystallization Tool	Crystallization Method	PDB IDs
Peptide	**δ-opioid** *mouse*	ΔN 1-35, ΔC 343-372, ΔICL3 245-250			T4L ICL3		LCP	4EJ4
	δ-opioid *human*	ΔN 1-35, ΔC 339-372		P37S (Xtal)	bRIL N-term		LCP	4N6H, 4RWA, 4RWD
	κ-opioid *human*	ΔN 2-42, ΔC 359-380, ΔICL3 S262		I135L (exp.)	T4L ICL3		LCP	4DJH
	μ-opioid *mouse*	ΔN 6-51, ΔC 361-398, ΔICL3 264-269			T4L ICL3		LCP	4DKL
	nociceptin/orphanin FQ *human*	ΔN 1-43, ΔC 341-370			bRIL N-term		LCP	4EA3
	PAR1 *human*	ΔN 1-85, ΔC 396-425, ΔICL3 V302		N250G (N-glyc.), N259S (N-glyc.)	T4L ICL3		LCP	3VW7
	orexin 2 *human*	ΔC 329-386, ΔICL3 255-293			glycogen synthase ICL3		LCP	4S0V

Class A								
Family	Receptor	Truncation	Stabilizing Mutations	Other Mutations	Chimera	Crystallization		PDB IDs
						Tool	Method	
Nucleotide – like	**adenosine A2A** *human*	ΔC 317-412, ΔICL3 209-221			T4L ICL3		LCP	3EML, 3QAK
		ΔC 317-412	L48A, A54L, T65A, Q89A	N154A (N-glyc.)			VD	2YDO, 2YDV
		ΔC 317-412	A54L, T88A, R107A, K122A, L202A, L235A, V239A, S277A	N154A (N-glyc.)			VD	3PWH, 3REY, 3RFM, 3UZA, 3UZC
		ΔC 317-412		N154Q (N-glyc.)		Fab2838	VD	3VG9
		ΔC 317-412, ΔICL3 210-217			bRIL ICL3		LCP	4EIY
	purinergic P2Y1 *human*	ΔICL3 248-252	D320N		rubredoxin ICL3		LCP	4XNV, 4XNW
	purinergic P2Y12 *human*		D294N		bRIL ICL3		LCP	4NTJ, 4PXZ, 4PY0
Lipid	**sphingosine-1-phosphate** *human*	ΔC 327-382, ΔICL3 232-244			T4L ICL3		LCP	3V2W, 3V2Y
	GPR40/FFAR1 *Human*	ΔICL3 211-212	L42A, F88A, G103A, Y202F		T4L ICL3		LCP	4PHU
	lysophosphatidic acid 1	ΔC 326-364			bRIL ICL3		LCP	4Z34, 4Z35
		ΔC 326-364		D204C, V282C (S-S)	bRIL ICL3		LCP	4Z36

Class A								
Family	Receptor	Truncation	Stabilizing Mutations	Other Mutations	Chimera	Crystallization Tool	Crystallization Method	PDB IDs
Rhodopsin *bovine*	WT						VD	1F88, 1HZX, 1L9H, 1U19, 1GZM, 2PED, 2G87, 2HPY, 3OAX
						Gta peptide	VD	3PQR, 3PXO, 4J4Q
						ArrFL-1 peptide	VD	4PFX
	stabilized		N2C, D282C (S-S)				VD	2J4Y
	constitutively active mutants		N2C, D282C (S-S)	E113Q (CAM)		Gta peptide	VD	2X72
			N2C, D282C (S-S)	M257Y (CAM)		Gta peptide	VD	4A4M
	disease mutants		N2C, D282C (S-S)	G90D (CAM)			VD	4BEZ
			N2C, D282C (S-S)	G90D (CAM)		Gta peptide	VD	4BEY
	opsin (apo)						VD	3CAP
	opsin (apo)					Gta peptide	VD	3DQB
Rhodopsin *squid*	*squid*						VD	2ZIY, 2Z73, 3AYN, 3AYM

NOTE: rhodopsin structures of poor resolution (> 3.5 Å; 2I35, 2I36, 2i37), and those obtained through reinterpretation of published data (3C9L, 3C9M) are not included in the table.

Class B							
Receptor	Truncation	Stabilizing Mutations	Other Mutations	Chimera	Crystallization Tool	Crystallization Method	PDB IDs
glucagon *human*	ΔN 1-122, ΔC 433-477			bRIL N-term		LCP	4L6R
corticotropin-releasing factor 1 *human*	ΔN 1-103, ΔC 374-444, ΔICL2 221-223	V120A, L144A, W156A, S160A, K228A, F260A, I277A, Y309A, F330A, S349A, Y363A		T4L ICL2		LCP	4K5Y

Class C							
Receptor	Truncation	Stabilizing Mutations	Other Mutations	Chimera	Crystallization Tool	Crystallization Method	PDB IDs
metabotropic glutamate type 1 *human*	ΔN 1-580, ΔC 861-1194			bRIL N-term		LCP	4OR2
metabotropic glutamate type 5 *human*	ΔN 2-568, ΔC 837-1153	E579A, N667Y, I669A, G675M, T742A, S753A		T4L ICL2		LCP	4OO9

Smoothened							
Receptor	Truncation	Stabilizing Mutations	Other Mutations	Chimera	Crystallization Tool	Crystallization Method	PDB IDs
smoothened *human*	ΔN 1-189, ΔC 556-787			bRIL N-term		LCP	4JKV, 4N4W
	ΔN 1-189, ΔC 556-787, ΔICL3 434-440			bRIL ICL3		LCP	4O9R, 4QIM, 4QIN

Viral GPCRs							
Receptor	Truncation	Stabilizing Mutations	Other Mutations	Chimera	Crystallization Tool	Crystallization Method	PDB IDs
chemokine US28 *human cytomegalovirus*						LCP	4XT3
	ΔN 1-9, ΔC 310-354				Nb7	LCP	4XT1

Supplementary Table 2. Ligand and mutagenesis data for selected GPCRs. Ligand data include the number of ligands found in the ChEMBLdb for each receptor (and how many of those are similar to the co-crystallized ligands). Mutation data include the number of ligands used in mutagenesis studies, the number of mutants and positions mutated, and the combination of mutants and ligands. See the footnotes for details.

GPCR	Ligand data			Mutagenesis data		
	chemical structure[a]	name[b]: PDBid	# total[c] [# similar[d]]	# of ligands in mutagenesis studies [# of protein ligands][e]	#mutants[f] [positions[g]]	#mutant-ligand comb.[h]
Aminergic receptors						
β_1AR	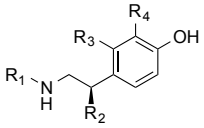	isoproterenol: 2Y03[1] salbutamol: 2Y04[1] dobutamine: 2Y00/2Y01[1] carmoterol: 2Y02[1]	1191 [106]	19	33 [27]	149[2]
	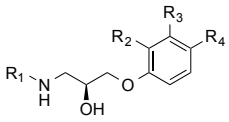	Carazolol: 2YCW[3] Carvedilol: 4AMJ[4] Bucindolol: 4AMI[4] Cyanopindolol: 2VT4[5]/ 2YCX[3]/2YCY[3]/4BVN[5] I-cyanopindolol: 2YCZ				
	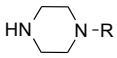	arylpiperazine 19: 3ZPQ[6] arylpiperazine 20: 3ZPR[6]				
β_2AR	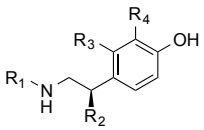	epinephrine: 4LDO[7] hydrox.bnz.isopr.:4LDL[7] BI-167107: 3P0G[8]/3SN6[9]/4LDE[7] FAUC50: 3PDS 4QKS[10]	1352 [187]	39	171 [91]	298[2]
	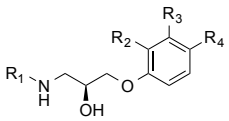	alprenolol: 3NYA[11] carazolol: 2RH1[12]/4GBR VS hit: 3NY9[11] ICI-118,551: 3NY8[11]				
	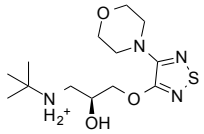	timolol: 3D4S[13]				
D_3R	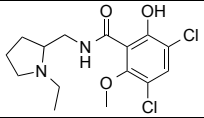	eticlopride: 3PBL[14]	2668 [18]	31	20 [18]	144[2]
M_2	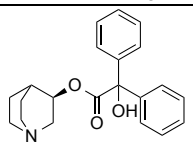	(*R*)-3-quinuclidinyl benzilate: 4MQS[15]	1546 [43]	38	41 [32][2]	207[2]
	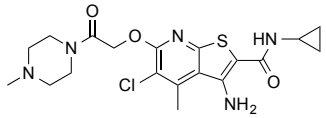	LY2119620: 4MQT[16]				
	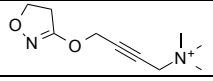	iperoxo: 4MQT[16]				

M_3	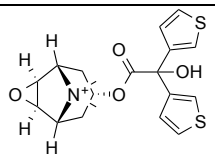	tiotropium: 4DAJ[17]/ 4U14[18]/4U15[18]/4U16[18]	1385 [15]	24	68 [55]	224[2]
H_1R	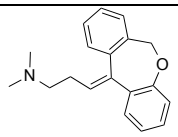	doxepin : 3RZE[19]	1201 [5]	31	28 [16]	238[2]
$5HT_{1B}$	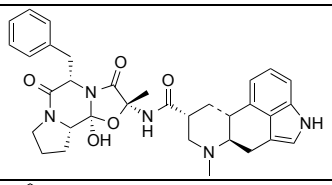	ergotamine: 4IAR[20,21]	1040 [2/253]	18	37 [23]	124[21-23]
		dihydroergotamine: 4IAQ[20,21]				
$5HT_{2B}$	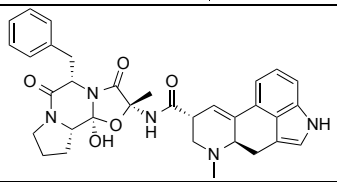	ergotamine: 4IB4[20,21]	1104 [11/64]☆	6	20 [20]	63[21-23]
Chemokine receptors						
CCR5	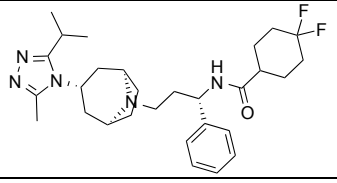	Maraviroc: 4MBS[24]	1793 [96]	26 [15]	148 [103]	1048[25,26]
CXCR4	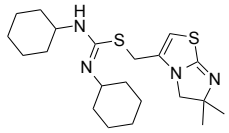	1T1t: 3ODU[24]	166 [18]	35 [19]	112 [86]	583[25,27]
	Peptide[a]	CVX15: 3OE0/3OE6/ 3OE8/3OE9[28]				
	Chemokine[a]	vMIP-II: 4RWS[29]				

Opioid receptors						
OPRD	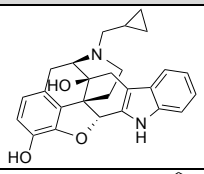	naltrindole: 4EJ4[31]/4N6H[32]	2461 [333]	44	67 [45][23,32]	340[23,32]
	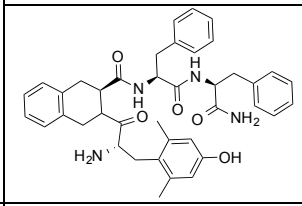	PRD_001256: 4RWA/4RWD[33]				
OPRM	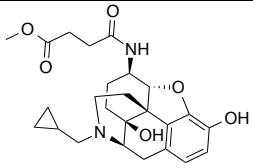	β-funaltrexamine: 4DKL[34]	2678 [198]	35	35 [25]	133[23]
OPRK	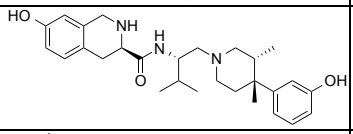	JDTic: 4DJH[35]	2755 [37]	26	45 [37]	119[23,35]
OPRX	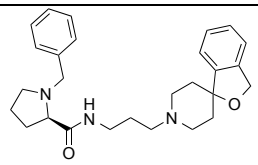	NFQ: 4EA3[36]	1078 [20]	25	12 [12]	48[23,36]
Adenosine receptors						
$A_{2A}R$	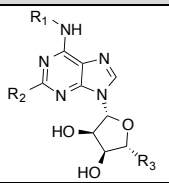	Adenosine: 2YDO[37] NECA: 2YDV[37] UK-432097: 3QAK[38]	3447 [556]	71	48 [32]	473[39]
	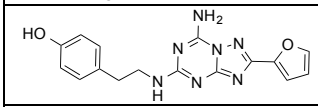	ZM241385: 3EML [40]/3PWH[41]/3VG9[42]/3VGA[42]				
	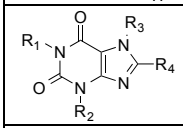	XAC: 3REY[41] caffeine: 3RFM [41]				
	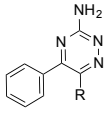	1,2,4-triazine 4g: 3UZA[43] 1,2,4-triazine 4e: 3UZC[43]				

Purinergic receptors						
P_2Y_{12}	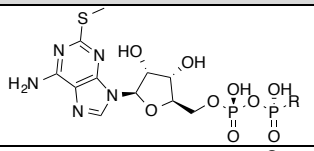	2MeSADP: 4PXZ[46] 2MeSATP: 4PY0[46]	906 [92]	3	10 [10]	$12^{39,46,47}$
	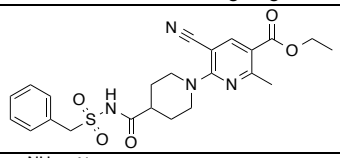	AZD1283: 4NTJ[47]				
P_2Y_1	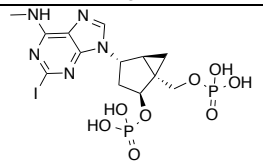	MRS2500: 4XNW[48]	301 [191]	4	53 [31]	$97^{39,48}$
	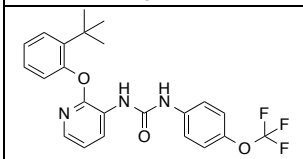	BPTU: 4XNV[48]				
Proteinase-activated receptors						
PAR1	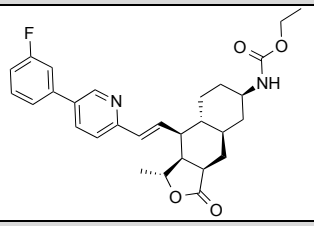	Vorapaxar: 3VW7[49]	574 [236]	1	3 [3]	5^{49}
Lipid receptors						
S1P1	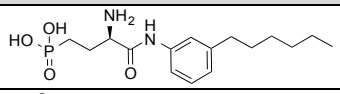	ML056: 3V2W[50]/3V2Y[50]	1241 [32]	14	53 [27]	$115^{50,51}$
FFAR1	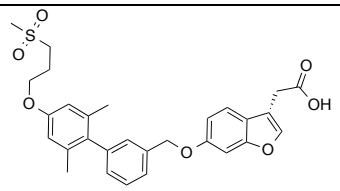	TAK-875: 4PHU[44]	539 [71]	7	15 [10]	$47^{44,45}$
Neurotensin receptors						
NTR1	Peptide[a]	NTS(8-13): 4GRV[50]/3ZEV[52]	253	7 [3]	56 [50]	131^{23}
Orexin receptors						
OX2R	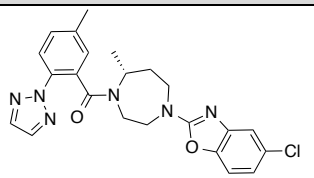	Suvorexant: 4S0V[53]	576 [52]	7 [3]	22 [21]	118

Secretin-like receptors						
CRF_1	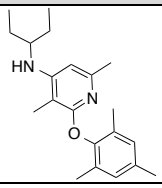	CP-376395: 4K5Y[54]	1404 [6]	20 [11]	185 [170]	289[54-56]
GCGR	-	4L6R[i) 57]	710	6 [5][57]	217 [145]	260[55]
Metabotropic glutamate receptors						
mGluR1	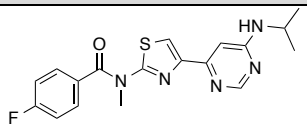	FITM: 4OR2[i 58]	476 [22][j]	12	37 [26]	90[X 59,60]
mGluR5	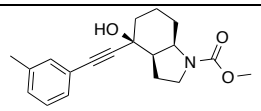	mavoglurant: 4OO9[i 60]	1415 [32][j]	16	70 [33]	253 [59,60]
Frizzled receptors						
SMO	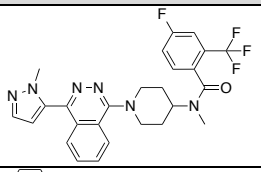	LY2940680: 4JKV[61]	355 [32]	16	13 [12]	58[60,62,63]
	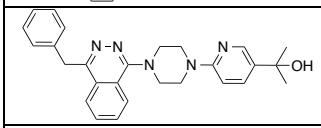	ANTA XV: 4QIM[63]				
	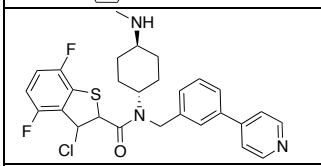	SAG1.5: 4QIN[63]				
	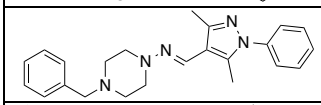	SANT-1: 4N4W[63]				
	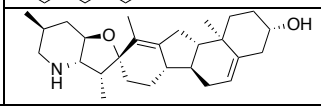	cyclopamine: 4O9R[63]				

[a)] Conserved scaffolds are shown for ligand series of β_1, β_2, $5HT_{1B}$, and A2A, while molecular structures of large co-crystallized polypeptide/protein ligands of CXCR4, US28, and NTR1 are not displayed; parts of the ligands with high B-factors are colored red;
[b)] Co-crystallized ligands that have been investigated in mutation studies are underlined (mutation data extracted from GPCRDB and indicated references);
[c)] Ligands (60 heavy atoms or lower) extracted from ChEMBLdb with binding affinity (IC_{50}/K_i) or functional potency (IC_{50}/EC_{50}) of at least 10 μM;
[d)] Number of ligands with ECFP-4 Tanimoto similarity ≥ 0.4 to a co-crystallized ligand of the corresponding receptor;
[e)] Number of unique ligands studied in mutation studies, protein ligands (60 heavy atoms or higher) indicated between brackets;
[f)] Number of unique mutants investigated in mutation studies;
[g)] Number of unique residue positions investigated in mutation studies;
[h)] Number of investigated combinations of mutants and ligands (mutation data extracted from GPCRDB and/or indicated references);
i) Similarity assessment only with co-crystallized ligands in 7TM domain (not ECD).

References

1. Warne, T.; Moukhametzianov, R.; Baker, J. G.; Nehme, R.; Edwards, P. C.; Leslie, A. G.; Schertler, G. F.; Tate, C. G. The structural basis for agonist and partial agonist action on a beta(1)-adrenergic receptor. *Nature* **2011,** 469, 241-4.
2. Kooistra, A. J.; Kuhne, S.; de Esch, I. J. P.; Leurs, R.; de Graaf, C. A structural chemogenomics analysis of aminergic GPCRs: lessons for histamine receptor ligand design. *Br J Pharmacol* **2013**.
3. Moukhametzianov, R.; Warne, T.; Edwards, P. C.; Serrano-Vega, M. J.; Leslie, A. G.; Tate, C. G.; Schertler, G. F. Two distinct conformations of helix 6 observed in antagonist-bound structures of a beta1-adrenergic receptor. *Proceedings of the National Academy of Sciences of the United States of America* **2011,** 108, 8228-32.
4. Warne, T.; Edwards, P. C.; Leslie, A. G.; Tate, C. G. Crystal structures of a stabilized beta1-adrenoceptor bound to the biased agonists bucindolol and carvedilol. *Structure* **2012,** 20, 841-9.
5. Miller-Gallacher, J. L.; Nehme, R.; Warne, T.; Edwards, P. C.; Schertler, G. F.; Leslie, A. G.; Tate, C. G. The 2.1 A Resolution Structure of Cyanopindolol-Bound beta1-Adrenoceptor Identifies an Intramembrane Na+ Ion that Stabilises the Ligand-Free Receptor. *PLoS One* **2014,** 9, e92727.
6. Christopher, J. A.; Brown, J.; Dore, A. S.; Errey, J. C.; Koglin, M.; Marshall, F. H.; Myszka, D. G.; Rich, R. L.; Tate, C. G.; Tehan, B.; Warne, T.; Congreve, M. Biophysical fragment screening of the beta1-adrenergic receptor: identification of high affinity arylpiperazine leads using structure-based drug design. *Journal of Medicinal Chemistry* **2013,** 56, 3446-55.
7. Ring, A. M.; Manglik, A.; Kruse, A. C.; Enos, M. D.; Weis, W. I.; Garcia, K. C.; Kobilka, B. K. Adrenaline-activated structure of beta-adrenoceptor stabilized by an engineered nanobody. *Nature* **2013**.
8. Rasmussen, S. G.; Choi, H. J.; Fung, J. J.; Pardon, E.; Casarosa, P.; Chae, P. S.; Devree, B. T.; Rosenbaum, D. M.; Thian, F. S.; Kobilka, T. S.; Schnapp, A.; Konetzki, I.; Sunahara, R. K.; Gellman, S. H.; Pautsch, A.; Steyaert, J.; Weis, W. I.; Kobilka, B. K. Structure of a nanobody-stabilized active state of the beta(2) adrenoceptor. *Nature* **2011,** 469, 175-80.
9. Rasmussen, S. G.; DeVree, B. T.; Zou, Y.; Kruse, A. C.; Chung, K. Y.; Kobilka, T. S.; Thian, F. S.; Chae, P. S.; Pardon, E.; Calinski, D.; Mathiesen, J. M.; Shah, S. T.; Lyons, J. A.; Caffrey, M.; Gellman, S. H.; Steyaert, J.; Skiniotis, G.; Weis, W. I.; Sunahara, R. K.; Kobilka, B. K. Crystal structure of the beta2 adrenergic receptor-Gs protein complex. *Nature* **2011,** 477, 549-55.
10. Weichert, D.; Kruse, A. C.; Manglik, A.; Hiller, C.; Zhang, C.; Hubner, H.; Kobilka, B. K.; Gmeiner, P. Covalent agonists for studying G protein-coupled receptor activation. *Proceedings of the National Academy of Sciences of the United States of America* **2014,** 111, 10744-8.
11. Wacker, D.; Fenalti, G.; Brown, M. A.; Katritch, V.; Abagyan, R.; Cherezov, V.; Stevens, R. C. Conserved binding mode of human beta2 adrenergic receptor inverse agonists and antagonist revealed by X-ray crystallography. *Journal of the American Chemical Society* **2010,** 132, 11443-5.
12. Cherezov, V.; Rosenbaum, D. M.; Hanson, M. A.; Rasmussen, S. G.; Thian, F. S.; Kobilka, T. S.; Choi, H. J.; Kuhn, P.; Weis, W. I.; Kobilka, B. K.; Stevens, R. C. High-resolution crystal structure of an engineered human beta2-adrenergic G protein-coupled receptor. *Science* **2007,** 318, 1258-65.
13. Hanson, M. A.; Cherezov, V.; Griffith, M. T.; Roth, C. B.; Jaakola, V. P.; Chien, E. Y.; Velasquez, J.; Kuhn, P.; Stevens, R. C. A specific cholesterol binding site is established by the 2.8 A structure of the human beta2-adrenergic receptor. *Structure* **2008,** 16, 897-905.
14. Chien, E. Y.; Liu, W.; Zhao, Q.; Katritch, V.; Han, G. W.; Hanson, M. A.; Shi, L.; Newman, A. H.; Javitch, J. A.; Cherezov, V.; Stevens, R. C. Structure of the human dopamine D3 receptor in complex with a D2/D3 selective antagonist. *Science* **2010,** 330, 1091-5.
15. Haga, K.; Kruse, A. C.; Asada, H.; Yurugi-Kobayashi, T.; Shiroishi, M.; Zhang, C.; Weis, W. I.; Okada, T.; Kobilka, B. K.; Haga, T.; Kobayashi, T. Structure of the human M2 muscarinic acetylcholine receptor bound to an antagonist. *Nature* **2012,** 482, 547-51.
16. Kruse, A. C.; Ring, A. M.; Manglik, A.; Hu, J.; Hu, K.; Eitel, K.; Hubner, H.; Pardon, E.; Valant, C.; Sexton, P. M.; Christopoulos, A.; Felder, C. C.; Gmeiner, P.; Steyaert, J.; Weis, W. I.; Garcia, K. C.; Wess, J.; Kobilka, B. K. Activation and allosteric modulation of a muscarinic acetylcholine receptor. *Nature* **2013,** 504, 101-6.
17. Kruse, A. C.; Hu, J.; Pan, A. C.; Arlow, D. H.; Rosenbaum, D. M.; Rosemond, E.; Green, H. F.; Liu, T.; Chae, P. S.; Dror, R. O.; Shaw, D. E.; Weis, W. I.; Wess, J.; Kobilka, B. K. Structure and dynamics of the M3 muscarinic acetylcholine receptor. *Nature* **2012,** 482, 552-6.
18. Thorsen, T. S.; Matt, R.; Weis, W. I.; Kobilka, B. K. Modified T4 Lysozyme Fusion Proteins Facilitate G Protein-Coupled Receptor Crystallogenesis. *Structure* **2014,** 22, 1657-1664.
19. Shimamura, T.; Shiroishi, M.; Weyand, S.; Tsujimoto, H.; Winter, G.; Katritch, V.; Abagyan, R.; Cherezov, V.; Liu, W.; Han, G. W.; Kobayashi, T.; Stevens, R. C.; Iwata, S. Structure of the human histamine H1 receptor complex with doxepin. *Nature* **2011,** 475, 65-70.
20. Wacker, D.; Wang, C.; Katritch, V.; Han, G. W.; Huang, X. P.; Vardy, E.; McCorvy, J. D.; Jiang, Y.; Chu, M.; Siu, F. Y.; Liu, W.; Xu, H. E.; Cherezov, V.; Roth, B. L.; Stevens, R. C. Structural features for functional selectivity at serotonin receptors. *Science* **2013,** 340, 615-9.
21. Wang, C.; Jiang, Y.; Ma, J.; Wu, H.; Wacker, D.; Katritch, V.; Han, G. W.; Liu, W.; Huang, X. P.; Vardy, E.; McCorvy, J. D.; Gao, X.; Zhou, X. E.; Melcher, K.; Zhang, C.; Bai, F.; Yang, H.; Yang, L.; Jiang, H.; Roth, B. L.; Cherezov, V.; Stevens, R. C.; Xu, H. E. Structural basis for molecular recognition at serotonin receptors. *Science* **2013,** 340, 610-4.
22. Shi, L.; Javitch, J. A. The binding site of aminergic G protein-coupled receptors: the transmembrane segments and second extracellular loop. *Annu Rev Pharmacol Toxicol* **2002,** 42, 437-67.
23. Isberg, V.; Vroling, B.; van der Kant, R.; Li, K.; Vriend, G.; Gloriam, D. GPCRDB: an information system for G protein-coupled receptors. *Nucleic Acids Res* **2014,** 42, D422-5.

24. Tan, Q.; Zhu, Y.; Li, J.; Chen, Z.; Han, G. W.; Kufareva, I.; Li, T.; Ma, L.; Fenalti, G.; Zhang, W.; Xie, X.; Yang, H.; Jiang, H.; Cherezov, V.; Liu, H.; Stevens, R. C.; Zhao, Q.; Wu, B. Structure of the CCR5 chemokine receptor-HIV entry inhibitor maraviroc complex. *Science* **2013,** 341, 1387-90.
25. Scholten, D. J.; Canals, M.; Maussang, D.; Roumen, L.; Smit, M. J.; Wijtmans, M.; de Graaf, C.; Vischer, H. F.; Leurs, R. Pharmacological modulation of chemokine receptor function. *Br J Pharmacol* **2012,** 165, 1617-43.
26. Garcia-Perez, J.; Rueda, P.; Alcami, J.; Rognan, D.; Arenzana-Seisdedos, F.; Lagane, B.; Kellenberger, E. Allosteric model of maraviroc binding to CC chemokine receptor 5 (CCR5). *J Biol Chem* **2011,** 286, 33409-21.
27. Kufareva, I.; Salanga, C. L.; Handel, T. M. Chemokine and chemokine receptor structure and interactions: implications for therapeutic strategies. *Immunol Cell Biol* **2015**.
28. Wu, B.; Chien, E. Y.; Mol, C. D.; Fenalti, G.; Liu, W.; Katritch, V.; Abagyan, R.; Brooun, A.; Wells, P.; Bi, F. C.; Hamel, D. J.; Kuhn, P.; Handel, T. M.; Cherezov, V.; Stevens, R. C. Structures of the CXCR4 chemokine GPCR with small-molecule and cyclic peptide antagonists. *Science* **2010,** 330, 1066-71.
29. Qin, L.; Kufareva, I.; Holden, L. G.; Wang, C.; Zheng, Y.; Zhao, C.; Fenalti, G.; Wu, H.; Han, G. W.; Cherezov, V.; Abagyan, R.; Stevens, R. C.; Handel, T. M. Structural biology. Crystal structure of the chemokine receptor CXCR4 in complex with a viral chemokine. *Science* **2015,** 347, 1117-22.
30. Burg, J. S.; Ingram, J. R.; Venkatakrishnan, A. J.; Jude, K. M.; Dukkipati, A.; Feinberg, E. N.; Angelini, A.; Waghray, D.; Dror, R. O.; Ploegh, H. L.; Garcia, K. C. Structural biology. Structural basis for chemokine recognition and activation of a viral G protein-coupled receptor. *Science* **2015,** 347, 1113-7.
31. Granier, S.; Manglik, A.; Kruse, A. C.; Kobilka, T. S.; Thian, F. S.; Weis, W. I.; Kobilka, B. K. Structure of the delta-opioid receptor bound to naltrindole. *Nature* **2012,** 485, 400-4.
32. Fenalti, G.; Giguere, P. M.; Katritch, V.; Huang, X. P.; Thompson, A. A.; Cherezov, V.; Roth, B. L.; Stevens, R. C. Molecular control of delta-opioid receptor signalling. *Nature* **2014,** 506, 191-6.
33. Fenalti, G.; Zatsepin, N. A.; Betti, C.; Giguere, P.; Han, G. W.; Ishchenko, A.; Liu, W.; Guillemyn, K.; Zhang, H.; James, D.; Wang, D.; Weierstall, U.; Spence, J. C.; Boutet, S.; Messerschmidt, M.; Williams, G. J.; Gati, C.; Yefanov, O. M.; White, T. A.; Oberthuer, D.; Metz, M.; Yoon, C. H.; Barty, A.; Chapman, H. N.; Basu, S.; Coe, J.; Conrad, C. E.; Fromme, R.; Fromme, P.; Tourwe, D.; Schiller, P. W.; Roth, B. L.; Ballet, S.; Katritch, V.; Stevens, R. C.; Cherezov, V. Structural basis for bifunctional peptide recognition at human delta-opioid receptor. *Nat Struct Mol Biol* **2015,** 22, 265-8.
34. Manglik, A.; Kruse, A. C.; Kobilka, T. S.; Thian, F. S.; Mathiesen, J. M.; Sunahara, R. K.; Pardo, L.; Weis, W. I.; Kobilka, B. K.; Granier, S. Crystal structure of the micro-opioid receptor bound to a morphinan antagonist. *Nature* **2012,** 485, 321-6.
35. Wu, H.; Wacker, D.; Mileni, M.; Katritch, V.; Han, G. W.; Vardy, E.; Liu, W.; Thompson, A. A.; Huang, X. P.; Carroll, F. I.; Mascarella, S. W.; Westkaemper, R. B.; Mosier, P. D.; Roth, B. L.; Cherezov, V.; Stevens, R. C. Structure of the human kappa-opioid receptor in complex with JDTic. *Nature* **2012,** 485, 327-32.
36. Thompson, A. A.; Liu, W.; Chun, E.; Katritch, V.; Wu, H.; Vardy, E.; Huang, X. P.; Trapella, C.; Guerrini, R.; Calo, G.; Roth, B. L.; Cherezov, V.; Stevens, R. C. Structure of the nociceptin/orphanin FQ receptor in complex with a peptide mimetic. *Nature* **2012,** 485, 395-9.
37. Lebon, G.; Warne, T.; Edwards, P. C.; Bennett, K.; Langmead, C. J.; Leslie, A. G.; Tate, C. G. Agonist-bound adenosine A2A receptor structures reveal common features of GPCR activation. *Nature* **2011,** 474, 521-5.
38. Xu, F.; Wu, H.; Katritch, V.; Han, G. W.; Jacobson, K. A.; Gao, Z. G.; Cherezov, V.; Stevens, R. C. Structure of an agonist-bound human A2A adenosine receptor. *Science* **2011,** 332, 322-7.
39. Jacobson, K. A.; Costanzi, S.; Deflorian, F. Probing GPCR structure: adenosine and P2Y nucleotide receptors. *Methods Enzymol* **2013,** 520, 199-217.
40. Jaakola, V. P.; Griffith, M. T.; Hanson, M. A.; Cherezov, V.; Chien, E. Y.; Lane, J. R.; Ijzerman, A. P.; Stevens, R. C. The 2.6 angstrom crystal structure of a human A2A adenosine receptor bound to an antagonist. *Science* **2008,** 322, 1211-7.
41. Dore, A. S.; Robertson, N.; Errey, J. C.; Ng, I.; Hollenstein, K.; Tehan, B.; Hurrell, E.; Bennett, K.; Congreve, M.; Magnani, F.; Tate, C. G.; Weir, M.; Marshall, F. H. Structure of the adenosine A(2A) receptor in complex with ZM241385 and the xanthines XAC and caffeine. *Structure* **2011,** 19, 1283-93.
42. Hino, T.; Arakawa, T.; Iwanari, H.; Yurugi-Kobayashi, T.; Ikeda-Suno, C.; Nakada-Nakura, Y.; Kusano-Arai, O.; Weyand, S.; Shimamura, T.; Nomura, N.; Cameron, A. D.; Kobayashi, T.; Hamakubo, T.; Iwata, S.; Murata, T. G-protein-coupled receptor inactivation by an allosteric inverse-agonist antibody. *Nature* **2012,** 482, 237-40.
43. Congreve, M.; Andrews, S. P.; Dore, A. S.; Hollenstein, K.; Hurrell, E.; Langmead, C. J.; Mason, J. S.; Ng, I. W.; Tehan, B.; Zhukov, A.; Weir, M.; Marshall, F. H. Discovery of 1,2,4-triazine derivatives as adenosine A(2A) antagonists using structure based drug design. *J Med Chem* **2012,** 55, 1898-903.
44. Srivastava, A.; Yano, J.; Hirozane, Y.; Kefala, G.; Gruswitz, F.; Snell, G.; Lane, W.; Ivetac, A.; Aertgeerts, K.; Nguyen, J.; Jennings, A.; Okada, K. High-resolution structure of the human GPR40 receptor bound to allosteric agonist TAK-875. *Nature* **2014,** 513, 124-7.
45. Tikhonova, I. G.; Sum, C. S.; Neumann, S.; Engel, S.; Raaka, B. M.; Costanzi, S.; Gershengorn, M. C. Discovery of novel agonists and antagonists of the free fatty acid receptor 1 (FFAR1) using virtual screening. *J Med Chem* **2008,** 51, 625-33.
46. Zhang, J.; Zhang, K.; Gao, Z. G.; Paoletta, S.; Zhang, D.; Han, G. W.; Li, T.; Ma, L.; Zhang, W.; Muller, C. E.; Yang, H.; Jiang, H.; Cherezov, V.; Katritch, V.; Jacobson, K. A.; Stevens, R. C.; Wu, B.; Zhao, Q. Agonist-bound structure of the human P2Y12 receptor. *Nature* **2014,** 509, 119-22.
47. Zhang, K.; Zhang, J.; Gao, Z. G.; Zhang, D.; Zhu, L.; Han, G. W.; Moss, S. M.; Paoletta, S.; Kiselev, E.; Lu, W.; Fenalti, G.; Zhang, W.; Muller, C. E.; Yang, H.; Jiang, H.; Cherezov, V.; Katritch, V.; Jacobson, K. A.; Stevens, R. C.; Wu, B.; Zhao, Q. Structure of the human P2Y12 receptor in complex with an antithrombotic drug. *Nature* **2014,** 509, 115-8.
48. Zhang, D.; Gao, Z. G.; Zhang, K.; Kiselev, E.; Crane, S.; Wang, J.; Paoletta, S.; Yi, C.; Ma, L.; Zhang, W.; Han, G. W.; Liu, H.; Cherezov, V.; Katritch, V.; Jiang, H.; Stevens, R. C.; Jacobson, K. A.; Zhao, Q.; Wu, B. Two disparate ligand-binding sites in the human P2Y receptor. *Nature* **2015**.

49. Zhang, C.; Srinivasan, Y.; Arlow, D. H.; Fung, J. J.; Palmer, D.; Zheng, Y.; Green, H. F.; Pandey, A.; Dror, R. O.; Shaw, D. E.; Weis, W. I.; Coughlin, S. R.; Kobilka, B. K. High-resolution crystal structure of human protease-activated receptor 1. *Nature* **2012,** 492, 387-92.
50. Hanson, M. A.; Roth, C. B.; Jo, E.; Griffith, M. T.; Scott, F. L.; Reinhart, G.; Desale, H.; Clemons, B.; Cahalan, S. M.; Schuerer, S. C.; Sanna, M. G.; Han, G. W.; Kuhn, P.; Rosen, H.; Stevens, R. C. Crystal structure of a lipid G protein-coupled receptor. *Science* **2012,** 335, 851-5.
51. Parrill, A. L.; Tigyi, G. Integrating the puzzle pieces: the current atomistic picture of phospholipid-G protein coupled receptor interactions. *Biochim Biophys Acta* **2013,** 1831, 2-12.
52. Egloff, P.; Hillenbrand, M.; Klenk, C.; Batyuk, A.; Heine, P.; Balada, S.; Schlinkmann, K. M.; Scott, D. J.; Schutz, M.; Pluckthun, A. Structure of signaling-competent neurotensin receptor 1 obtained by directed evolution in Escherichia coli. *Proc Natl Acad Sci U S A* **2014,** 111, E655-62.
53. Yin, J.; Mobarec, J. C.; Kolb, P.; Rosenbaum, D. M. Crystal structure of the human OX2 orexin receptor bound to the insomnia drug suvorexant. *Nature* **2015,** 519, 247-50.
54. Hollenstein, K.; Kean, J.; Bortolato, A.; Cheng, R. K.; Dore, A. S.; Jazayeri, A.; Cooke, R. M.; Weir, M.; Marshall, F. H. Structure of class B GPCR corticotropin-releasing factor receptor 1. *Nature* **2013,** 499, 438-43.
55. Hollenstein, K.; de Graaf, C.; Bortolato, A.; Wang, M. W.; Marshall, F. H.; Stevens, R. C. Insights into the structure of class B GPCRs. *Trends Pharmacol Sci* **2014,** 35, 12-22.
56. Coin, I.; Katritch, V.; Sun, T.; Xiang, Z.; Siu, F. Y.; Beyermann, M.; Stevens, R. C.; Wang, L. Genetically encoded chemical probes in cells reveal the binding path of urocortin-I to CRF class B GPCR. *Cell* **2013,** 155, 1258-69.
57. Siu, F. Y.; He, M.; de Graaf, C.; Han, G. W.; Yang, D.; Zhang, Z.; Zhou, C.; Xu, Q.; Wacker, D.; Joseph, J. S.; Liu, W.; Lau, J.; Cherezov, V.; Katritch, V.; Wang, M. W.; Stevens, R. C. Structure of the human glucagon class B G-protein-coupled receptor. *Nature* **2013,** 499, 444-9.
58. Dore, A. S.; Okrasa, K.; Patel, J. C.; Serrano-Vega, M.; Bennett, K.; Cooke, R. M.; Errey, J. C.; Jazayeri, A.; Khan, S.; Tehan, B.; Weir, M.; Wiggin, G. R.; Marshall, F. H. Structure of class C GPCR metabotropic glutamate receptor 5 transmembrane domain. *Nature* **2014,** 511, 557-62.
59. Gregory, K. J.; Conn, P. J. Molecular Insights into Metabotropic Glutamate Receptor Allosteric Modulation. *Mol Pharmacol* **2015**.
60. Wu, H.; Wang, C.; Gregory, K. J.; Han, G. W.; Cho, H. P.; Xia, Y.; Niswender, C. M.; Katritch, V.; Meiler, J.; Cherezov, V.; Conn, P. J.; Stevens, R. C. Structure of a class C GPCR metabotropic glutamate receptor 1 bound to an allosteric modulator. *Science* **2014,** 344, 58-64.
61. Wang, C.; Wu, H.; Katritch, V.; Han, G. W.; Huang, X. P.; Liu, W.; Siu, F. Y.; Roth, B. L.; Cherezov, V.; Stevens, R. C. Structure of the human smoothened receptor bound to an antitumour agent. *Nature* **2013,** 497, 338-43.
62. Hoch, L.; Faure, H.; Roudaut, H.; Schoenfelder, A.; Mann, A.; Girard, N.; Bihannic, L.; Ayrault, O.; Petricci, E.; Taddei, M.; Rognan, D.; Ruat, M. MRT-92 inhibits Hedgehog signaling by blocking overlapping binding sites in the transmembrane domain of the Smoothened receptor. *FASEB J* **2015**.
63. Wang, C.; Wu, H.; Evron, T.; Vardy, E.; Han, G. W.; Huang, X. P.; Hufeisen, S. J.; Mangano, T. J.; Urban, D. J.; Katritch, V.; Cherezov, V.; Caron, M. G.; Roth, B. L.; Stevens, R. C. Structural basis for Smoothened receptor modulation and chemoresistance to anticancer drugs. *Nat Commun* **2014,** 5, 4355.

MOL #99663

Supplementary files to generate the images in Figure 3.

3eml_density.pml	PyMOL commands to generate Figure 3, top left panel
3eml_lig_density.pml	PyMOL commands to generate Figure 3, bottom left panel
4eiy_density.pml	PyMOL commands to generate Figure 3, top right panel
4eiy_lig_density.pml	PyMOL commands to generate Figure 3, bottom right panel

In order to run successfully these scripts in PyMOL:

1. Download the files containing the crystallographic structure and the electron density map of each protein. These files can be obtained by navigating, respectively to the Protein Data Bank (PDB) (http://www.pdb.org) and the Electron Density Server (EDS) at Uppsala University (http://eds.bmc.uu.se/eds/), searching for each PDB code (in this case, 3EML and 4EIY), and looking for the 'Download' sections.

In the EDS, in order to generate a 'standard' map for visual inspection of the experimental electron density, download the 2mFo-DFc map in CCP4 format. Once downloaded, rename the files to '3eml_map.ccp4' and '4eiy_map.ccp4'.

These files (3eml.pdb, 3eml_map.ccp4, 4eiy.pdb, 4eiy_map.ccp4) need to be in the same directory where the scripts will be executed.

2. Initiate a PyMOL session and move to the directory where the structure and electron density files are located by using the command 'cd' in the command line section of the PyMOL window; e.g.

```
> cd /Users/johndoe/Documents/Structures
```

(See http://www.pymolwiki.org/index.php/Practical_Pymol_for_Beginners for a basic tutorial on PyMOL).

3. Run the script by typing its name preceded by the symol ‘@, in the command line section of PyMOL; e.g.

```
> @3eml_density.pml
```

These scripts can be opened with any text editor, and modified to obtain different images.

MOL #99663

Supplementary files to generate the images in Figure 4.

3eml_bfactors.pml	PyMOL commands to generate Figure 4, left panel
4eiy_bfactors.pml	PyMOL commands to generate Figure 4, right panel

In order to run successfully these scripts in PyMOL:

1. Download the files containing the crystallographic structure of each protein. These files can be obtained by navigating to the Protein Data Bank (PDB) (http://www.pdb.org), searching for each PDB code (in this case, 3EML and 4EIY), and looking for the 'Download' section.

These files (3eml.pdb, 4eiy.pdb) need to be in the same directory where the scripts will be executed.

2. Initiate a PyMOL session and move to the directory where the structure files are located by using the command 'cd' in the command line section of the PyMOL window; e.g.

```
> cd /Users/johndoe/Documents/Structures
```

(See http://www.pymolwiki.org/index.php/Practical_Pymol_for_Beginners for a basic tutorial on PyMOL).

3. Run the script by typing its name preceded by the symol '@, in the command line section of PyMOL; e.g.

```
> @3eml_bfactors.pml
```

These scripts can be opened with any text editor, and modified to obtain different images.